

# ZAP70 interaction with 13 mRNAs as a potential immunotherapeutic target for endometrial cancer

YUMING ZHANG, HAI'OU LU and YUEXIN YU

Department of Reproductive Medicine, General Hospital of Northern Theater Command,  
Shenyang, Liaoning 110016, P.R. China

Received August 29, 2022; Accepted March 17, 2023

DOI: 10.3892/ol.2023.13799

**Abstract.** For advanced, refractory endometrial cancer (EC), it is advisable to find effective immunotherapeutic targets. In the present study, genes affecting the immune status of uterine corpus endometrial carcinoma (UCEC) samples within The Cancer Genome Atlas were explored by weighted correlation network analysis and differential gene expression analysis. The protein function and immune correlation of 14 key genes, including  $\zeta$ -chain-associated protein kinase 70 (ZAP70), were analyzed. Based on the expression levels of key genes, the patients with UCEC were divided into two groups using consensus clustering, low expression (group 1) and high expression (group 2). Next, the functions of differentially expressed genes (DEGs) between the two groups were identified using Gene Ontology enrichment analysis, Kyoto Encyclopedia of Genes and Genomes analysis and Gene Set Enrichment Analysis. The immune status of the patients in the two groups was evaluated using immune infiltration score and the expression levels of targets of immune checkpoint inhibitors. The role of ZAP70 in the prognosis of patients with UCEC and the differences in ZAP70 expression between EC tissues and healthy intimal tissues were determined by reverse transcription-quantitative PCR and immunohistochemistry. The present study found strong correlations between key genes, including ZAP70, LCK, FOXP3, TIGIT, CTLA4, ICOS, CD5, IL2RG, PDCD1, TNFRSF4, CD27, CCR7, GZMB, CXCL9. From the enrichment analyses, it was found that the functions of these DEGs were related to T cells. Patients in group 2 had stronger immune infiltration and higher immune checkpoints expression compared with those in group 1. ZAP70 was expressed at higher levels in EC tissues compared with in normal tissues, and may act as a protective factor in EC. In conclusion, ZAP70 interaction with 13 mRNAs may affect

the immune status of patients with EC and may be a potential target for immunotherapy.

## Introduction

Endometrial cancer (EC) is the sixth most frequent cancer type in women, and its incidence and mortality rates have increased in recent years (1). From 1987 to 2014, the cases of EC increased by 75% globally and the mortalities associated with EC increased by 300% (2,3). For patients without distant metastasis, surgery is usually followed by post-operative adjuvant therapy (4). Hormone therapy may be used to protect patients with well-differentiated EC who wish to reproduce (4). At present, there are few effective anticancer drugs for EC; thus, it is urgent to develop novel molecular targeted drugs for EC (5).

Cancer treatment has markedly changed in the past decade with the development of tumor immunotherapy (6). EC responds well to immunotherapy compared with other solid tumors owing to its unique immune properties, such as a high tumor mutation load (7). In The Cancer Genome Atlas (TCGA), EC is divided into four molecular subtypes: i) DNA Polymerase  $\epsilon$  (POLE) mutation, ii) microsatellite instability-high/mismatch repair deficient (MSI-H/dMMR), iii) high copy number and iv) low copy number. POLE mutation is associated with high-grade histology, but prognosis for this type of EC is good (8). As this type of EC has a strong immune response, it is the most suitable type for immunotherapy (9). Programmed death-ligand 1 (PD-L1) is expressed in 92% of EC cases; it is indicative of advanced stage and poor tumor differentiation. Patients with chemotherapy-resistant, metastatic EC have high response rates to programmed death-1 (PD-1) and PD-L1 inhibitors (10). The upregulated expression of CTLA-4, LAG-3 and IDO in POLE tumors suggests potential in immunotherapy of POLE tumors (11). Recently, additional immune checkpoints have been identified such as TIGIT and CD73, which will help to investigate the mechanism and efficacy of immune checkpoint inhibitors (ICIs) in EC treatment (12,13).

$\zeta$ -Chain-associated protein kinase 70 (ZAP70) is a tyrosine kinase that binds to the T-cell receptor (TCR) complex, and acts on the TCR-mediated signaling pathway in thymocytes and peripheral T cells (14). *In vivo*, ITAM is dephosphorylated and ZAP70 is in a resting state when the

---

*Correspondence to:* Professor Yuexin Yu, Department of Reproductive Medicine, General Hospital of Northern Theater Command, 83 Wenhua Road, Shenyang, Liaoning 110016, P.R. China  
E-mail: ghntcyx@163.com

**Key words:** endometrial cancer, T cell, prognosis, immune checkpoint inhibitors, immunotherapy

major histocompatibility complex-binding antigenic peptide fragment (pMHC) of the pathogen or tumor is not recognized by the TCR. When pMHC on a tumor or pathogen is recognized by the TCR, tyrosine-protein kinase LCK on CD4 binds to ITAM, phosphorylating ITAM, and ZAP70 is activated when it binds to phosphorylated ITAM (15). Previous studies on ZAP70 have been restricted primarily to chronic lymphocytic leukemia (CLL), with limited detailed research on solid tumors (16,17). For example, high expression of ZAP70 in CLL is related to non-mutated IgVH, malignant progression of the disease and poor total survival rate (18). Since the majority of ZAP70 is found in  $\alpha\beta$  and  $\gamma\delta$  T cells, natural killer (NK) cells and a few immature B cells, the systemic side effects of treatment targeting ZAP70 are manageable (19).

In the present study, transcriptome and clinical data from patients with EC were downloaded from TCGA. According to the results of weighted gene co-expression network analysis (WGCNA) analysis, 14 key genes, including ZAP70, were identified. The patients were divided into two groups according to the expression levels of key genes (high vs. low), and the DEGs expressed in the two groups were identified. The differences in gene function, immune cell infiltration and ICI expression, as well as the prognosis of patients, between the two groups were analyzed by bioinformatics.

## Materials and methods

**Data sources and pre-processing.** The normalized RNA expression data and clinical characteristics (including age, status, FIGO stage and survival time) of 587 patients with EC were downloaded from TCGA (portal.gdc.cancer.gov) database (TCGA-UCEC) with the help of TCGAbiolinks R package (2.18.0), which included 552 tumor and 35 normal samples (20). Transcriptome data were transformed by  $\log_2(\text{FPMK}+1)$  (Fragments Per Kilobase of exon per Million fragments mapped) (21).

**DEGs between EC and normal samples.** DEGs were obtained by comparing htseq-counts data between tumor specimens and normal specimens using the R package DESeq2 (22). The threshold of screening DEGs was set as  $|\log_2(\text{foldchange})| > 1$  and  $P < 0.05$ .

**Immune-related key modules and hub genes screened by WGCNA.** Immune-related key modules and hub genes were screened using WGCNA (23). First, a soft threshold was determined and the coexpression similarity was raised to this threshold to calculate the adjacency. The soft threshold was calculated by the criterion of approximate scale-free topology. Second, the network structure was adjusted into topological overlap matrix after the adjacency association was determined, and genes with similar expression characteristics were clustered hierarchically. Third, the dynamic tree cutting algorithm was used to divide the modules, so that each module had  $\geq 20$  genes and the similar modules were fused (24). Finally, after constructing the network, immune-related modules and genes were obtained by adjusting the criteria of mode-trait correlation, gene significance (Pearson's correlation coefficient between genes and traits) and module membership (Pearson's

correlation coefficient between genes and module feature genes). As a result, an immune-related key module and hub genes were identified.

**Functional enrichment analysis.** Biological function analyses included Gene Ontology (GO) (geneontology.org/), Kyoto Encyclopedia of Genes and Genomes (KEGG) (genome.jp/kegg/) and Gene Set Enrichment Analysis (GSEA) (25). KEGG analyzed the cells metabolic pathways and functional pathways of gene enrichment. The top 20 pathways with the lowest P-value were identified and arranged according to their P-value (from smallest to largest) to focus on the most statistically significant pathways. GSEA was used to calculate the enrichment of known signaling pathways in specific rankings (26).

**Correlation analysis.** The Search Tool for the Retrieval of Interacting Genes/Proteins database was used to construct protein-protein interaction (PPI) networks (27); the confidence score was set to 0.700. Univariate Cox risk analysis was performed on survival status and survival time using the 'survival' package, and key genes affecting the survival status of patients with uterine corpus EC (UCEC) were identified (28). Spearman's correlations between gene and gene, between genes and ESTIMATEScore, and between genes and the single sample Gene Set Enrichment Analysis (ssGSEA) were calculated using the R package corrplot (0.84) (github.com/taiyun/corrplot). ESTIMATEScore is used to predict tumor purity and the presence of infiltrating stromal cells and immune cells in tumor tissue. This analysis estimates the ratio of stromal cells and immune cells in malignant tumor tissue based on gene expression data.

**Consensus clustering.** Patients with UCEC were divided into two groups using the R package ConsensusClusterPlus (1.54.0), and DEGs were obtained using the R package limma (29,30). The patients with UCEC were divided into two groups by consensus clustering based on transcriptome data of key genes in TCGA-UCEC samples, aiming to cluster the samples with similar expression levels of the key genes into one group.

**Evaluation of the immune microenvironment.** The R package, Estimation (1.0.13), was used to calculate and compare the StromalScore (stromal content), ImmuneScore (degree of immune cell infiltration), ESTIMATEScore (synthetic marks for stroma and immune) and TumorPurity (proportion of cancer cells in the admixture) of patients with UCEC (31). The proportion of 22 (B cells naive, B cells memory, Plasma cells, T cells CD8, T cells CD4 naive, T cells CD4 memory resting, T cells CD4 memory activated, T cells follicular helper, T cells regulatory (Tregs), T cells gamma delta, NK cells resting, NK cells activated, Monocytes, Macrophages M0, Macrophages M1, Macrophages M2, Dendritic cells resting, Dendritic cells activated, Mast cells resting, Mast cells activated, Eosinophils, Neutrophils) and 28 (Activated B cell, Activated CD4 T cell, Activated CD8 T cell, Activated dendritic cell, CD56bright natural killer cell, CD56dim natural killer cell, Central memory CD4 T cell, Central memory CD8 T cell, Effector memory CD4 T cell, Effector memory CD8 T cell, Eosinophil, Gamma delta T cell, Immature B cell, Immature

dendritic cell, Macrophage, Mast cell, MDSC, Memory B cell, Monocyte, Natural killer cell, Natural killer T cell, Neutrophil, Plasmacytoid dendritic cell, Regulatory T cell, T follicular helper cell, Type 1 T helper cell, Type 17 T helper cell, Type 2 T helper cell) immune cell types in each UCEC samples were analyzed using the R package Cibersort (v1.03) and Gene Set Variation Analysis (GSVA), respectively (32,33).

**Verification of key gene expression.** To verify the expression of 14 key genes in EC and normal endometrial tissue, the present study attempted to integrate the normal endometrial samples from the Genotype-Tissue Expression (GTEx) (<http://commonfund.nih.gov/GTEx/>) Project with EC samples from TCGA database. A total of 101 normal endometrial samples and 181 EC samples were obtained. The aforementioned 14 key genes were searched on PubMed ([pubmed.ncbi.nlm.nih.gov/](https://pubmed.ncbi.nlm.nih.gov/)) and the Web of Science (<https://www.webofscience.com/wos/>) to look for genes that have not been reported in EC or endometrium for further study.

**Patients.** Tissue samples were collected from patients who visited the Department of Obstetrics and Gynecology of General Hospital of Northern Theater Command (Shenyang, China) between January 2019 and December 2021. Tumoral tissue from 19 patients with EC and normal endometrial tissue from 11 patients with non-endometrial disease and non-cancer were collected and used to detect the mRNA expression levels of ZAP70 by reverse transcription-quantitative PCR (RT-qPCR). A comparison of age and BMI between patients with EC and patients with non-endometrial disease and non-cancer is presented in Table I. Paired EC and normal endometrial tissues from 10 patients with EC were used for immunohistochemical detection of ZAP70 protein expression. The clinicopathological characteristics of all patients with EC were shown in Table II.

**RT-qPCR.** Tissue RNA from 19 patients with EC and 11 patients with non-endometrial disease and non-cancer was extracted from ground tissues using TRIzol<sup>®</sup> reagent (Invitrogen; Thermo Fisher Scientific, Inc.). RNA was reverse transcribed into cDNA using the PrimeScript<sup>™</sup> RT Reagent Kit with gDNA Eraser (cat. no. RR047A; Takara Bio, Inc.) according to the manufacturer's protocol. cDNA was added to a 20- $\mu$ l system containing SYBR Premix Ex Taq (cat. no. RR820A; Takara Bio, Inc.). qPCR was performed using QuantStudio<sup>™</sup> 1 Real-Time PCR System (cat. no. A40425; Thermo Scientific, Inc.), and the thermocycling conditions were set as: 1 cycle of pre-denaturation (95°C for 30 sec), 40 cycles of PCR reaction (95°C 5 sec, 60°C 34 sec), and 1 cycle of solubilization curve analysis (95°C 15 sec, 60°C 60 sec, 95°C 15 sec). ZAP70 and GAPDH primer sequences are provided in Table III. The relative expression was expressed by  $2^{-\Delta\Delta C_q}$ , and the data were normalized to GAPDH (34). All experiments were repeated three times.

**Immunohistochemistry and immunofluorescence.** Fresh tissues were fixed at 4°C with 4% paraformaldehyde for 24 h and embedded in paraffin blocks. The 2-step plus Poly-HRP Anti Rabbit/Mouse IgG Detection System immunohistochemistry kit (cat. no. E-IR-R211; Elabscience Biotechnology, Inc.)

Table I. General characteristics of patients with endometrial cancer and healthy control patients.

Patient	Age, years (mean $\pm$ SD)	BMI, kg/m <sup>2</sup> (mean $\pm$ SD)
Endometrial cancer	50.68 $\pm$ 7.543	22.96 $\pm$ 3.275
Healthy control	53.18 $\pm$ 5.930	23.45 $\pm$ 2.826
P-value	0.3550	0.6833

Table II. Clinicopathological characteristics of patients with endometrial cancer.

Clinicopathological characteristic	Patients (n=19)	Percentage
Age, years		
<50	7	36.80
$\geq$ 50	12	63.20
BMI, kg/m <sup>2</sup>		
<25	14	73.70
$\geq$ 25	5	26.30
History of estrogen use		
Yes	2	10.50
None	17	89.50
FIGO stage		
I and II	12	63.20
III and IV	7	36.80
Survival status		
Alive	18	94.70
Deceased	1	5.30

Table III. Primer sequences used for reverse transcription-quantitative PCR.

Gene	Primer sequence (5' to 3')
ZAP70	F: CAAGTTTGACACGCTCTGGC R: GTAGGGGCTCTCATACACGC
GAPDH	F: CGGATTTGGTCGTATTGGG R: CTGGAAGATGGTGATGGGATT

ZAP70,  $\zeta$ -chain-associated protein kinase 70.

was used to analyze tissue sections (4  $\mu$ m). The experiment was conducted according to the kit instructions. The slides were incubated overnight at 4°C with rabbit anti-ZAP70 polyclonal antibody (1:200; E-AB-19063; Elabscience Biotechnology, Inc.). Five visual fields were randomly selected for each section under a 400x microscope for scoring, and the criteria were as follows: 1. According to staining intensity, the sections were divided into non-staining, light yellow, brown

and brown, which were recorded as 0, 1, 2 and 3 points in turn; 2. According to the percentage of colored cells in the field of vision, the positive cell rate was <10% : 1 point, 10-50% : 2 points, and >50% was rated as 3 points. The product of the two scores gives the final score. HEC-1-A (cat. no CL-0099; Procell Life Science & Technology Co., Ltd.) and Ishikawa (cat. no. CL-0283; Procell Life Science & Technology Co., Ltd.) cells were cultured in RPMI 1640 (cat. no SH30255.01; HyClone Biotechnology, Inc.) with 10% fetal bovine serum (FBS) (cat. no 164210; Procell Life Science & Technology Co., Ltd.). Cells were cultured under sterile conditions at 37°C and 5% CO<sub>2</sub>. Cells were fixed on coverslips, washed, permeabilized, sealed, and incubated with rabbit anti-ZAP70 polyclonal antibody (1:200; E-AB-19063; Elabscience Biotechnology, Inc.). Immunofluorescence Staining Kit-Anti-Rabbit Alexa Fluor 647 (cat. no. P0180; Beyotime Institute of Biotechnology) was used for testing the following day according to the manufacturer's protocol. Slides were examined and images captured under a fluorescence microscope (cat. no. 703548; Nikon Corporation).

**Statistical analysis.** Data were analyzed with R software (4.0.2) (<https://www.r-project.org/>), and GraphPad Prism version 8.0 (Dotmatics) was used to evaluate statistical difference. All hypothesis tests were two-sided, and  $P < 0.05$  was considered to indicate a statistically significant difference. Kaplan-Meier analysis was calculated using the R package 'glmnet' and compared by log-rank analysis. Wilcoxon rank-sum test was used to compare unpaired samples, whereas paired samples of immunohistochemistry were compared using Wilcoxon signed-rank test. Correlations were calculated with Spearman's coefficient analysis.

## Results

**Differential expression analysis and identification of immune hub genes by WGCNA.** WGCNA was performed on 6,131 genes that differed between EC and normal tissue from TCGA-UCEC (Fig. 1A). The soft threshold was set to 4 and the DEGs were clustered into 14 modules (Fig. 1B and C). Modules are highly interrelated clusters of genes with similar ESTIMATEScores. ESTIMATEScores of all samples are presented in the form of a heat map in order to obtain the module with the strongest correlation with immune score in the TCGA-UCEC sample (Fig. 1D). In the correlation heat map, 'ME magenta' represented the strongest correlation module with ImmuneScores ( $R = 0.93$ ;  $P < 0.001$ ; Fig. 1E). Finally, 108 hub genes which have high connectivity in the magenta module were screened according to module membership ( $MM > 0.5$ ) and gene significance ( $GS > 0.5$ ) (Fig. 1F). Module membership refers to the correlation between each gene and the module characteristics of a given module according to its gene expression profile. Gene significance is a measure of the importance of a gene. The higher the absolute value of GS of a gene, the greater its biological significance. The cut-off values of MM and GS are customized according to the distribution and number of hub genes in the module.

**Functional enrichment analysis and identification of 108 hub genes.** GO analysis of the 108 hub genes revealed that several

were enriched in 'T cell activation' and 'lymphocyte differentiation' ( $P < 0.001$ ; Fig. 2A). Through KEGG enrichment, it was found that the top three enrichment pathways of the 108 hub genes were 'Cytokine-cytokine receptor interaction', 'Osteoclast differentiation' and 'Th17 cell differentiation' ( $P < 0.001$ ; Fig. 2B). A PPI network was established, and 20 genes with closely related functions (yellow) were identified (Fig. 2C). Cox proportional hazards model found 14 genes that affect the survival outcome and survival time of patients with UCEC (Fig. 2D); ZAP70, LCK, FOXP3, TIGIT, CTLA4, ICOS, CD5, IL2RG, PDCD1, TNFRSF4, CD27, CCR7, GZMB and CXCL9 were identified as key genes that may affect the prognosis of patients with EC. Through gene-gene Spearman's correlation analysis, a strong positive correlation between these proteins encoded by key genes was found (Fig. 2E). Of these, ZAP70 has the strongest correlation with CD5. Regarding the correlation between genes and immune cell infiltration, the 14 key genes were positively associated with ImmuneScore and negatively associated with TumorPurity (Fig. 2F); of the key genes, IL2RG had the strongest correlation with ImmuneScore (Fig. 2F). ssGSEA show that, among the 28 immune cell types, the 14 key genes mainly affected activated CD8<sup>+</sup> T cells, immature B cells and Myeloid-derived suppressor cells (Fig. 2G). To determine whether these key genes were associated with a good prognosis in patients with UCEC, Kaplan-Meier analyses were performed. The median expression of key genes in each TCGA-UCEC sample was used as the cut-off point to separate the patients into high and low group. The results showed that patients with UCEC with higher expression of each key gene had a longer overall survival time (Fig. 3).

**Functional enrichment analysis of DEGs.** According to the results of consensus clustering, expression of each key gene in group 2 was higher compared with that in group 1 (Fig. 4A and B). There were 763 DEGs with statistically significant differences between patients of groups 1 and 2 (Fig. 4C). GSEA revealed that 'adaptive immune response', 'immune response regulating cell surface receptor signaling', 'lymphocyte differentiation', 'positive regulation of cytokine production' and 'T cell activation' were enriched (Fig. 4D). 'T cell activation', 'regulation of T cell activation', 'regulation of cell-cell adhesion' in GO term enrichment analysis (Fig. 4E), and 'Cytokine-cytokine receptor interaction', 'Viral protein interaction with cytokine and cytokine receptor' and 'Chemokine signaling pathway' in KEGG pathway enrichment analysis (Fig. 4F) revealed the role of DEGs in tumor development, immunity and other biological processes.

**Difference in immune cell infiltration and expression analysis of immune checkpoints.** ESTIMATE, CIBERSORT and ssGSEA analyses were used to determine the differences in the degree and composition of immune cell infiltration between the two groups. The higher StromalScore (Fig. 5A), ImmuneScore (Fig. 5B) and ESTIMATEScores (Fig. 5C), and lower TumorPurity (Fig. 5D) in group 2 compared with group 1 attested to a stronger degree of immune cell infiltration. The percentages of activated CD4<sup>+</sup> and CD8<sup>+</sup> T cells which are the main cells that play an antitumor role in group 2 were higher compared with group 1 in the 22 immune cell species from CIBERSORT and in the 28 immune cell infiltration assays



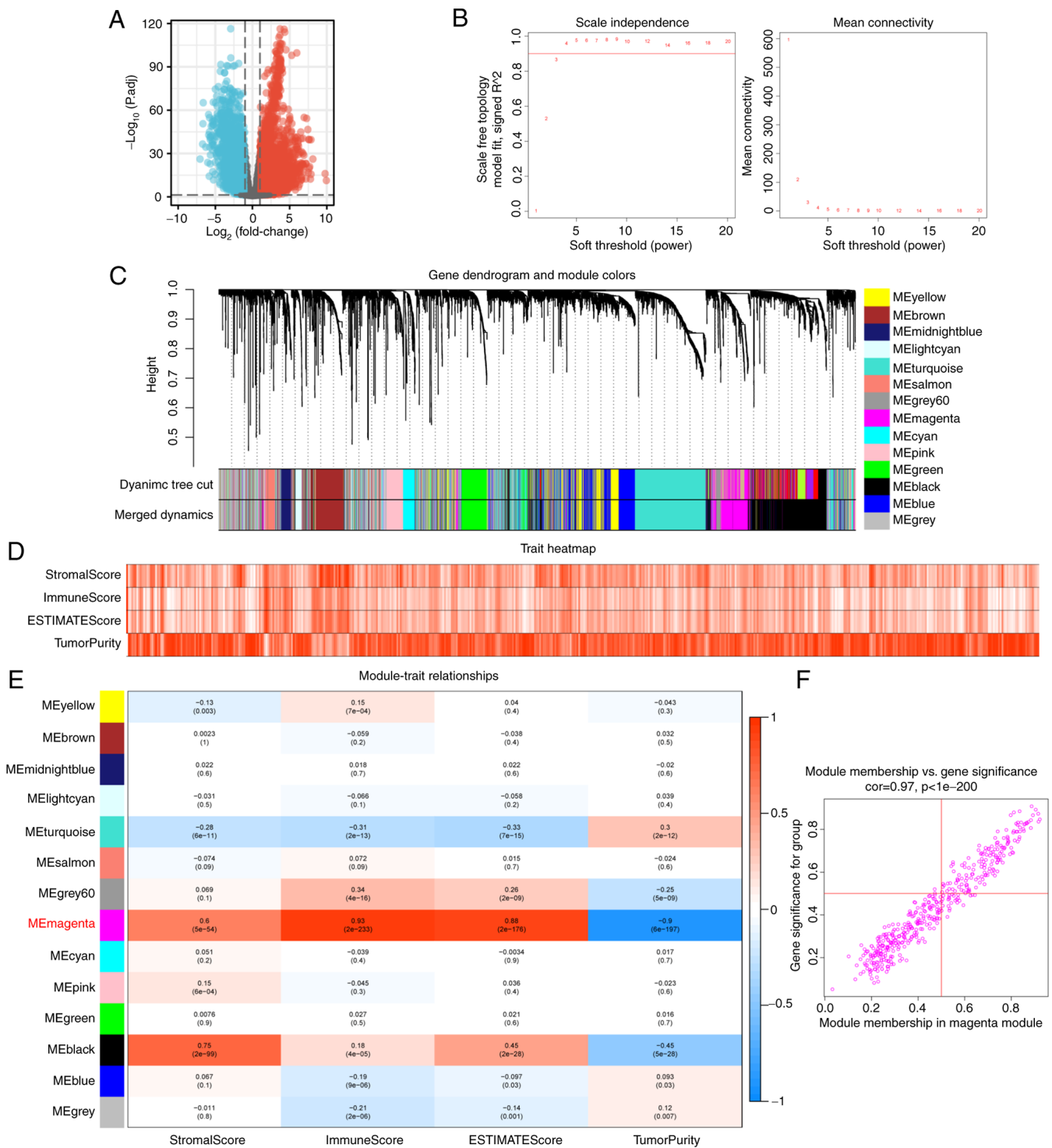


Figure 1. Identification of hub genes associated with EC immunity by using weighted gene co-expression network analysis. (A) Differentially expressed genes between EC and normal tissues. (B) Threshold of 4 was selected for creating the network topology. (C) Gene dendrogram and module colors. (D) ESTIMATE results of UCEC samples are shown in trait heatmap, with darker colors representing higher scores. (E) Genes in the magenta module had the strongest gene-ESTIMATE positive correlation. (F) Genes in the magenta module were selected according to module membership  $>0.5$  and gene significance  $>0.5$ . EC, endometrial cancer.

from ssGSEA (Fig. 5E and F, respectively). The expression levels of immune checkpoint markers usually determine the sensitivity of patients to immunotherapy. Notably, immune checkpoints markers PD1, PD-L1, PD-L2, CTLA-4, CD80, CD86, LAG3, TIM3, TIGIT, OX40, GITR, 4-1BB, ICOS, CD40, CD27 and CD70 were upregulated in group 2 compared with their expression levels in group 1 (Fig. 6).

*Verification of expression levels of ZAP70 in tissue and cells and its effect on prognosis.* Next, the expression of 14 key genes were examined in patients with UCEC from the GTEx-TCGA database. With the exception of ZAP70 and CCR7 (Fig. S1A and S1L), the expression of the other key genes was significantly higher in EC tissues compared with expression in normal tissues (Fig. S1). The aforementioned 14

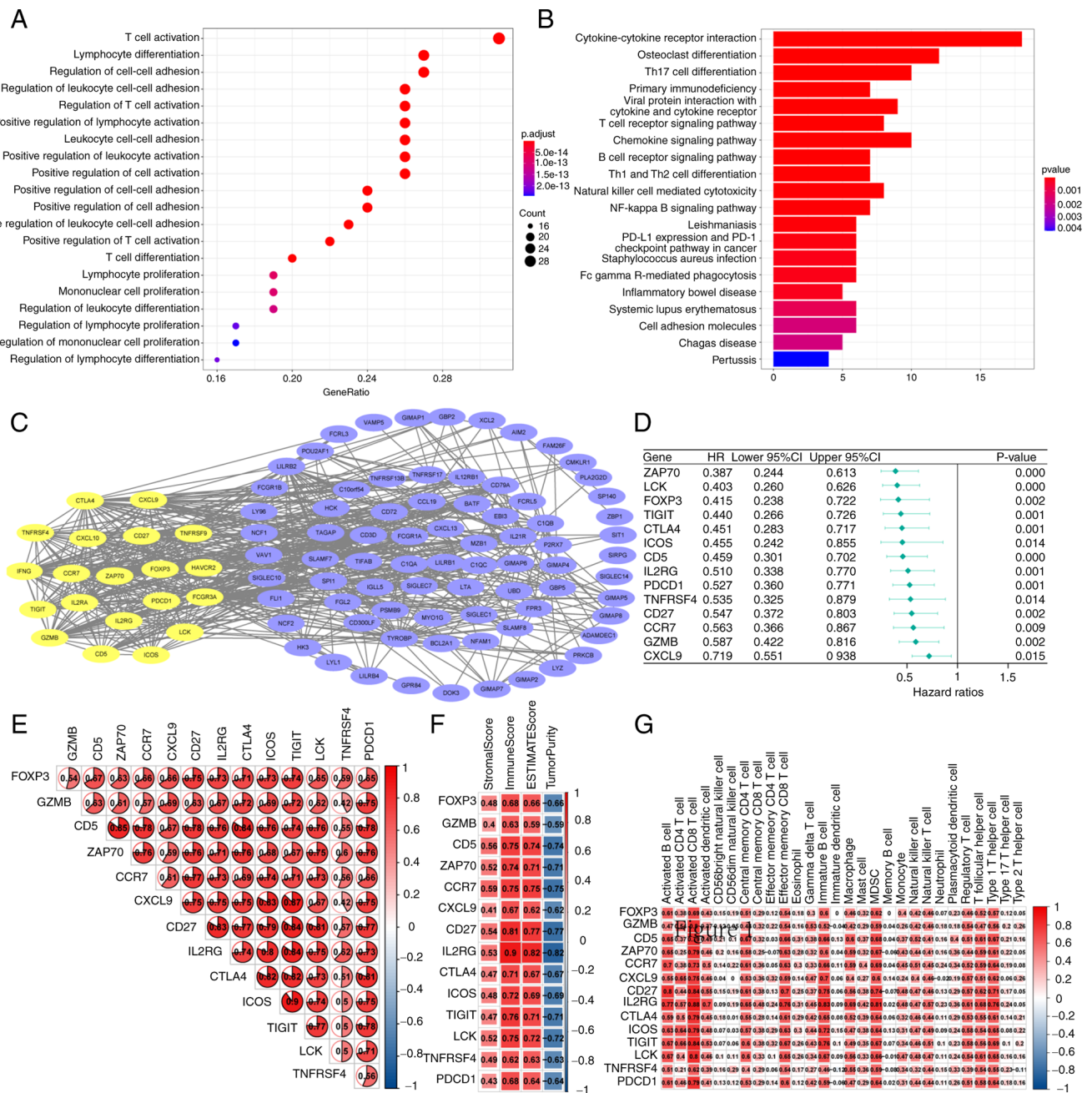


Figure 2. GO and KEGG enrichment analysis of 108 hub genes and identification of 14 key genes. (A) GO enrichment analysis of the hub genes. (B) KEGG pathway enrichment analysis of the hub genes. (C) Protein-protein interaction analysis found genes that interacted with each other. (D) Cox proportional hazards model was used to screen key genes. (E) Gene-gene correlation analysis. (F) Correlation between key genes and ESTIMATEScore. (G) Correlation between key genes and ssGSEA. GO, Gene Ontology; HR, hazard ratio; KEGG, Kyoto Encyclopedia of Genes and Genomes; ZAP70,  $\zeta$ -chain-associated protein kinase 70; ssGSEA, single sample Gene Set Enrichment Analysis.

key genes were searched on PubMed and the Web of Science. In addition to ZAP70, 13 other key genes were found to have been reported in normal endometrium or EC (35-46). Therefore, ZAP70 was selected for the subsequent experimental verification because to the best of our knowledge, it has not been reported in EC or endometrial tissue and thus represents a novel target. Subsequently, ZAP70 mRNA expression was examined in 19 EC tissues and 11 healthy endometrial tissues. It was shown that ZAP70 mRNA expression in EC tissues was higher than that in healthy endometrial tissues (Fig. 7A). Next, ZAP70 protein expression was detected in 10 pairs of EC and healthy endometrial tissues using

immunohistochemistry. Consistent with the mRNA expression levels, ZAP70 protein was 2.3 times more expressed in EC than in matched healthy endometrial tissue (Fig. 7B). This difference in expression could be attributed to the improved breadth rather than the accuracy of GTEx-TCGA data). The immunofluorescence assay data showed that ZAP70 was mainly expressed in the nucleus of EC cells, with limited expression in the cytoplasm (Fig. 7C). In TCGA database, the expression level of ZAP70 in EC tissues was higher than that in normal endometrial tissues (Fig. 7D). ZAP70 was expressed lower in patients with FIGO stage III and IV EC compared with those with FIGO stage I and II EC (Fig. 7E).

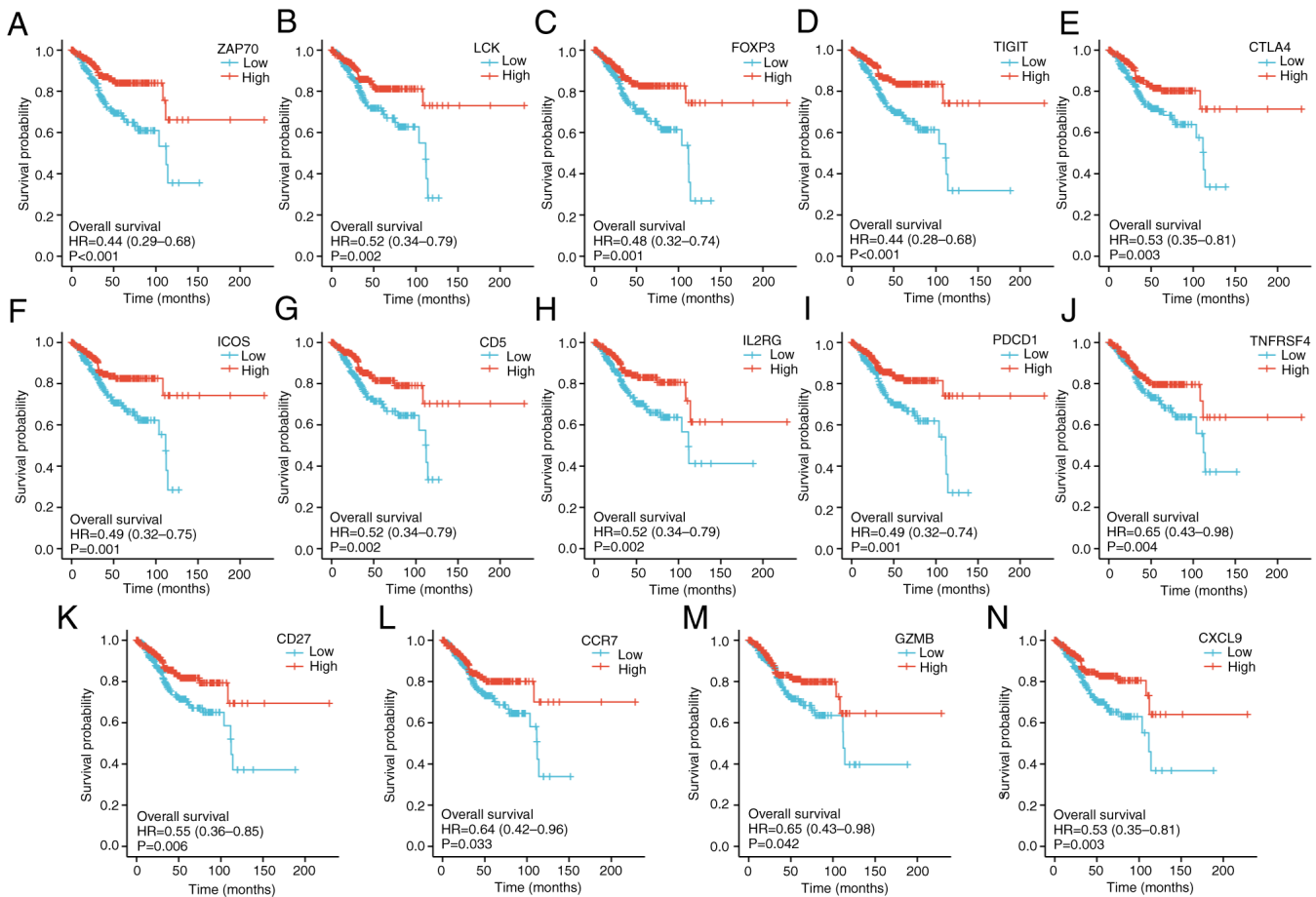


Figure 3. Kaplan-Meier survival curve analysis was used to determine the effects of 14 key genes on survival time of patients with uterine corpus endometrial cancer. Kaplan-Meier survival curve analysis of (A) ZAP70; (B) LCK; (C) FOXP3; (D) TIGIT; (E) CTLA4; (F) ICOS; (G) CD5; (H) IL2RG; (I) PDCD1; (J) TNFRSF4; (K) CD27; (L) CCR7; (M) GZMB; (N) CXCL9. HR, hazard ratio; ZAP70,  $\zeta$ -chain-associated protein kinase 70.

ZAP70 expression was lower in deceased patients than in those patients that were alive (Fig. 7F). In the correlation analysis between ZAP70 and ICIs using TCGA-UCEC data, it was found that ZAP70 was positively associated with 16 known immune checkpoints (Fig. 8).

## Discussion

The identification of immune checkpoints has overturned the model of cancer treatment and ushered in a new era of cancer treatment; however, only a small number of patients with cancer benefit from immune checkpoint therapy (47). Anti-PD-1/PD-L1 have been widely studied in MSI-H/dMMR EC, and their effects are encouraging. For example, in the KEYNOTE-158 trial, 49 patients with MSI-H EC with metastatic/relapsed disease were treated with pembrolizumab (PD-1 inhibitor), with an overall response rate (ORR) of 57%, a median progression-free survival (PFS) of 25.7 months, and a complete response in 16.3% of patients (48). In an efficacy study of durvalumab (anti-PD-L1) in patients with advanced EC, the ORR in the MMR-deficient group was 40% (n=35; 95%CI, 26-56), including 4 cases of complete response and 10 cases of partial response (49). The emergence of additional immunotherapeutic targets for advanced and refractory EC is expected.

The current study involved WGCNA on 6,131 genes that differed between cancer and normal tissues, and the magenta module, which contained 108 hub genes, demonstrated the strongest correlation with immune score. Through screening by PPI network and univariate Cox risk analysis, 14 key genes including ZAP70 were identified. ZAP70 is highly expressed in a wide variety of tumors (16). In hematological tumors, particularly CLL, ZAP70 enhances the phosphorylation of ZAP70-positive CLL B cells Syk, BLNK and PLC $\gamma$ , thereby promoting B cell receptor (BCR) signal enhancement, cell proliferation and migration to the tumor microenvironment (TME) (50,51). In contrast to CLL, in solid tumors, high ZAP70 expression indicates good prognosis and radiotherapy sensitivity (52). ZAP70 has been shown to be a potential therapeutic target in the TME affecting prognosis in laryngeal phosphorous cell carcinoma, breast cancer, prostate cancer, cutaneous melanoma, bladder cancer and nasopharyngeal cancer (53-58). In a novel chimeric antigen receptor (CAR) strategy for targeting NK cells, activation of Syk/ZAP70 reversed HLA-G mediated immunosuppression and restored NK cell lysis to ablate solid tumors (59).

In the present study, 108 immune-related DEGs were examined and the functional enrichment pathways were associated with T-cell activation and function in GO analysis. T cells are the main component of TME, and numerous

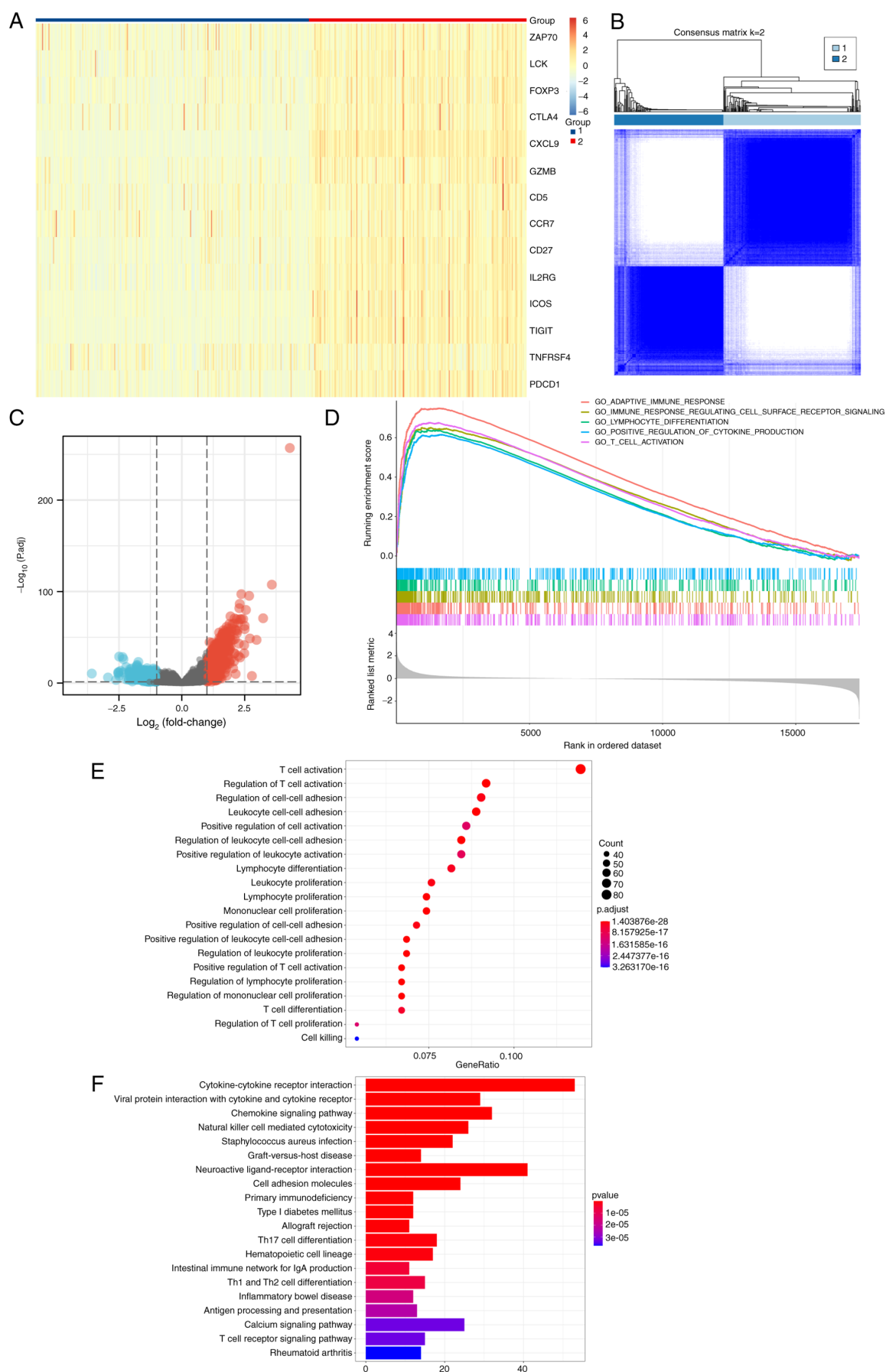


Figure 4. Consensus clustering and Enrichment analysis. (A) Heatmap of key genes expressed in TCGA-UCEC samples. (B) When set consensus matrix  $K=2$ , the groups of samples can be well distinguished, so TCGA-UCEC samples were divided into two groups. (C) DEGs between two groups of TCGA-UCEC samples after consensus clustering. (D) GSEA, (E) Gene Ontology and (F) Kyoto Encyclopedia of Genes and Genomes analysis of DEGs. DEGs, differentially expressed genes; P.adj, adjusted P-value.

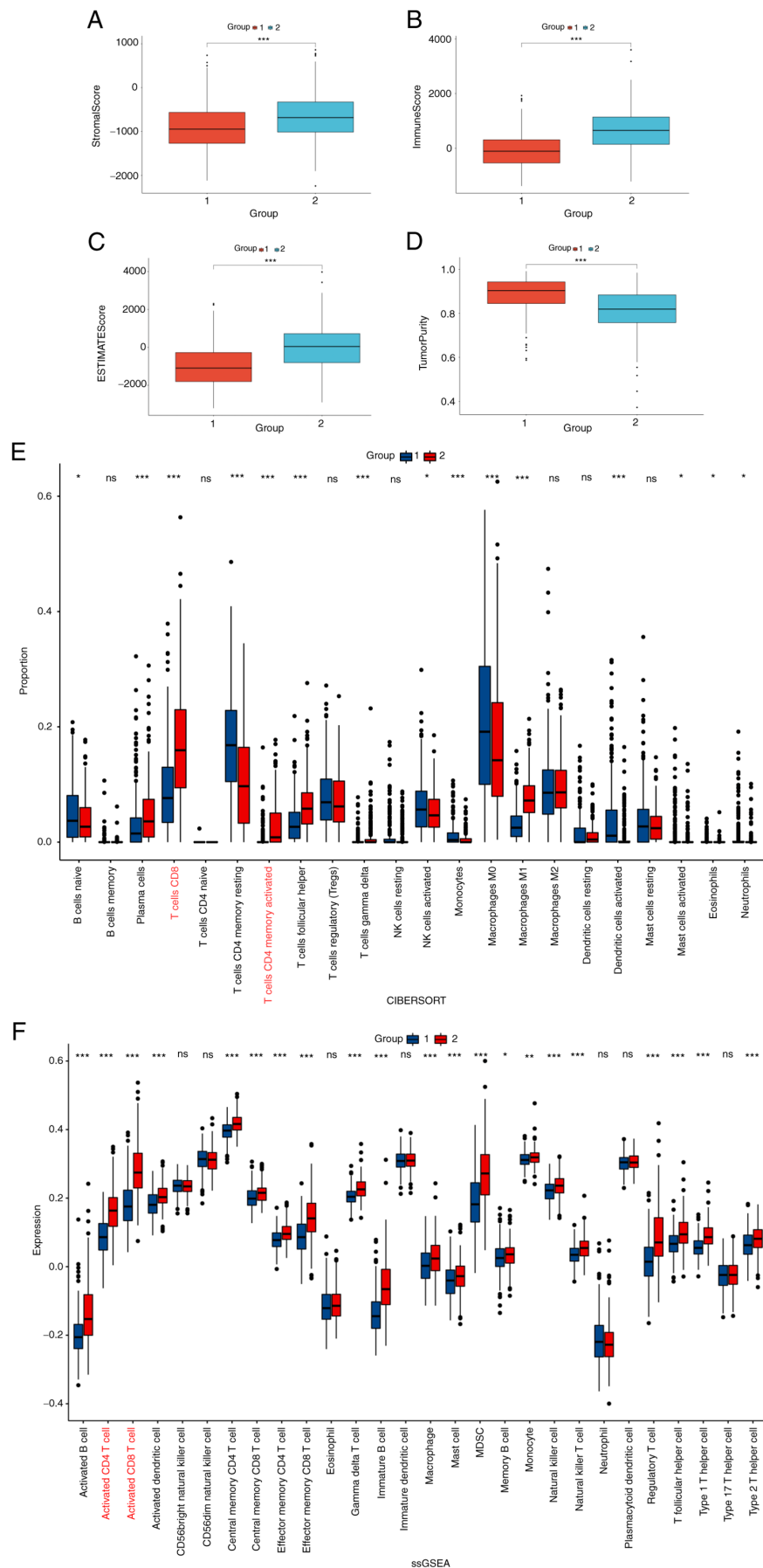


Figure 5. Immune cell infiltration analysis. Comparison of (A) StromaScore, (B) ImmuneScore, (C) ESTIMATEScore and (D) TumorPurity between two groups. (E) Differences in the proportion of 22 infiltrating immune cells between the two groups using CIBERSORT. (F) Differences in the proportion of 28 infiltrating immune cells between two groups infiltration using ssGSEA. ssGSEA, single sample Gene Set Enrichment Analysis; NK, natural killer; ns, not significant. \*P<0.05, \*\*P<0.01 and \*\*\*P<0.001.



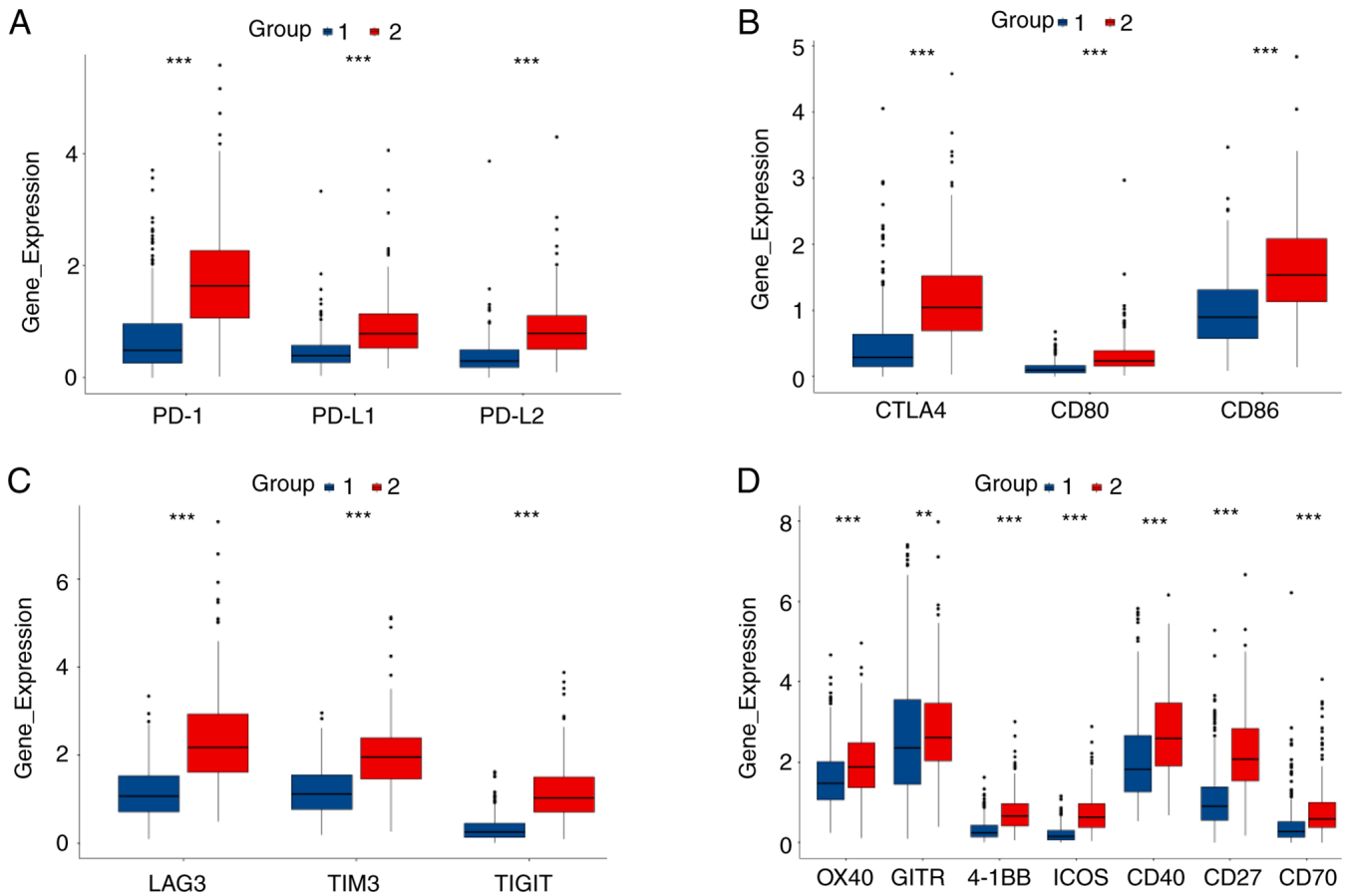


Figure 6. Comparison of the expression levels of immune checkpoint genes between two groups. (A) Comparison of PD-1, PD-L1 and PD-L2 expression levels between two groups. (B) Comparison of CTLA4, CD80 and CD86 expression levels between two groups. (C) Comparison of LAG3, TIM3 and TIGIT expression levels between two groups. (D) Comparison of OX40, GITR, 4-1BB, ICOS, CD40, CD27 and CD70 expression levels between two groups. PD1, programmed death 1; PD-L, programmed death ligand. \*\*P<0.01 and \*\*\*P<0.001

studies have been conducted on targeted therapy using T cells (60,61). Adoptive T-cell therapy (ACT) is the first and most effective treatment to target the immune system. This therapy involves *in vitro* amplification, screening and modification of autologous lymphocytes reinjection to the patient to achieve T cell-mediated tumor regression (62). Currently, research is being carried out to promote the use of ACT for the treatment of EC. To identify the factors influencing the prognosis of patients with UCEC, the present study used the univariate Cox risk analysis to identify 14 genes that may be protective factors: ZAP70, LCK, FOXP3, TIGIT, CTLA4, ICOS, CD5, IL2RG, PDCD1, TNFRSF4, CD27, CCR7, GZMB and CXCL9. Of these, ZAP70 had the highest association with CD5, which has been demonstrated in previous studies. Gladkikh *et al* (63) demonstrated that ZAP70 was differentially expressed in normal B lymphocytes with CD5-high and CD5-low expression, and low ZAP70 expression would lead to BCR signal dysfunction, which confirmed its key role in altered BCR signaling in B-CLL. When exploring the correlation between these key genes and the immune micro-environment, it was demonstrated that IL2RG was the most strongly associated gene with the ImmuneScore. IL2RG is located on Xq13 of the X chromosome and its mutation causes X-linked severe combined immunodeficiency (64). A defect in the IL2RG gene causes a lack of T, NK and partially

functional B cells, and this defect is fatal (65). Two classical immune checkpoints were observed in these key genes, PD-1 and CTLA4. In 2017, Le *et al* (66) examined the sensitivity of patients with advanced dMMR cancer to pembrolizumab treatment in 12 different tumor types. Of all the tumor types, dMMR occurred most frequently in EC (17%), with an ORR of 53% and a complete response rate of 21%, including 15 EC cases. Oh and Chae (67) reported a case of a patient with MMR-proficient, PD-L1-negative stage IV EC who was treated with combined inhibition of PD-1 and CTLA-4. The patient showed a marked response to the treatment shortly after treatment, with multiple tumor metastases being reduced.

The present study performed consensus clustering analysis based on the expression levels of 14 key genes in order to divide patients with UCEC into two groups for comparison. Functional enrichment analysis of DEGs in these two groups was associated with T-cell-mediated immune pathways. In the KEGG analysis, one of the pathways, 'Neuroactive ligand-receptor interaction', was absent from the top three. However, there are  $\geq 40$  DEGs of the 763 DEGs involved in this pathway. Previous studies have shown that the interaction between neuroactive ligands and receptors, as a part of the TME, affects tumor progression and invasion (68). Although there are no clear studies showing that nerve signaling can



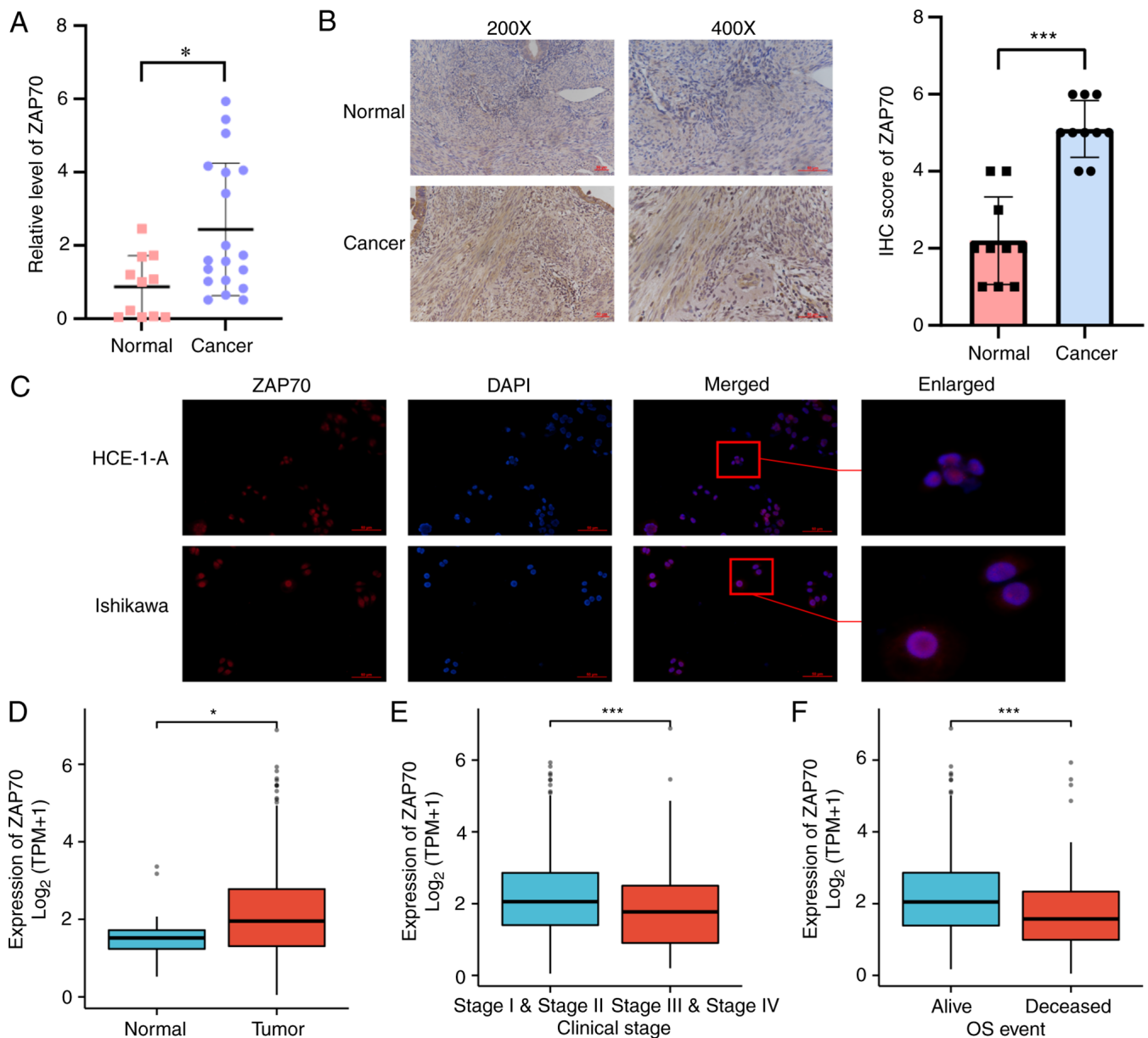


Figure 7. *In vivo* and *in vitro* validation of ZAP70 expression and its potential role in prognosis. (A) ZAP70 mRNA expression was detected in tissues by reverse transcription-quantitative PCR. (B) ZAP70 protein expression was detected in tissues by immunohistochemistry. Image intake was presented through the microscope (cat. no. 703548; Nikon Corporation). (C) Localization of ZAP70 in cells was detected using immunofluorescence (400x). Image intake was presented through the microscope (cat. no. 703548; Nikon Corporation). Differences in ZAP70 between (D) healthy and tumoral tissues, (E) FIGO clinical stages I/II and stages III/IV, and (F) living and deceased patients. IHC, immunohistochemistry; OS, overall survival; TPM, transcripts per kilobase million; ZAP70,  $\zeta$ -chain-associated protein kinase 70. \* $P < 0.05$  and \*\*\* $P < 0.001$ .

affect the immune microenvironment of patients with EC, the role of neuro-related genes in the reclassification of EC has been previously suggested (69). These findings indicated that neuroactive ligand receptor interactions in the TME may be used as a new research direction for immunotherapy of EC in the future.

Following consensus clustering of patients with UCEC in the present study, it was found that patients in group 2 with higher expression of key genes had higher immune cell infiltration status, particularly CD4<sup>+</sup> and CD8<sup>+</sup> T cells. CD8<sup>+</sup> T cells are the main effector cells of adaptive immunity against cancer cells in the microenvironment. However, during tumor development, CD8<sup>+</sup> T cells differentiate into a 'dysfunctional' state (70). As these cells are less reactive to

tumor antigens, cancer cells cannot be recognized and eliminated (71). Activation of CD8<sup>+</sup> T cells and intranodal migration of memory T cells are critical for cancer immunosurveillance, and these can be achieved by PD-1/PD-L1 inhibition or CAR T-cell therapy (72,73). The key genes LCK and ZAP70 have a direct impact on CAR T-cell therapy. Mestermann *et al* (74) showed that tyrosine kinase inhibitors can interfere with LCK, thereby inhibiting the phosphorylation of CD3 $\xi$  and ZAP70 $\xi$ . Inhibition of activated modules in the CAR structures, such as CD28-CD3 $\xi$  or 4-1BB-CD3 $\xi$ , resulted in functional inhibition of CD8<sup>+</sup> and CD4<sup>+</sup> CAR T cells. Based on these studies on immune cell infiltration and immune checkpoints, it can be speculated that patients with high expression of key genes, such as ZAP70, may be more suitable for CAR T-cell therapy.

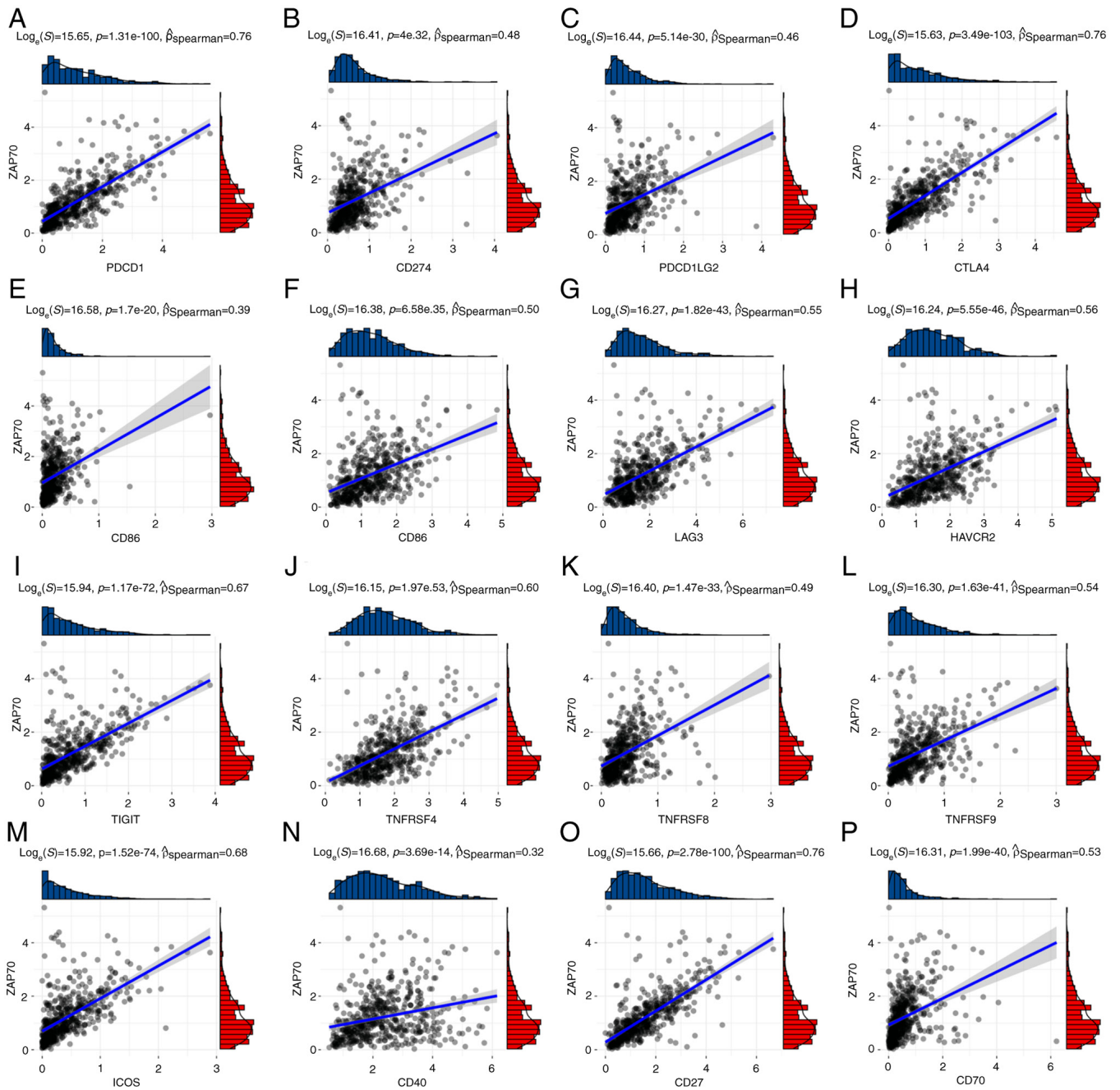


Figure 8. Correlation analysis between the expressions of ZAP70 and 16 known immune checkpoints in patients with uterine corpus endometrial cancer. Correlation analysis of ZAP70 and (A) PDCD1; (B) CD274; (C) PDCD1LG2; (D) CTLA4; (E) CD80; (F) CD86; (G) LAG3; (H) HAVCR2; (I) TIGIT; (J) TNFRSF4; (K) TNFRSF8; (L) TNFRSF9; (M) ICOS; (N) CD40; (O) CD27; (P) CD70 expression in TCGA-UCEC samples. ZAP70,  $\zeta$ -chain-associated protein kinase 70.

Finally, the expression and prognostic value of ZAP70 in EC were detected by combining experimental and TCGA-UCEC clinical data. First, high expression of ZAP70 mRNA and protein in EC tissues was confirmed by RT-qPCR and immunohistochemistry, respectively. However, the number of samples we used for this result was low, which makes our conclusion have certain limitations; thus, additional tissue samples are needed for further research on the functions of ZAP70 in EC. ZAP70 was positively associated with known ICIs, indicating that high expression of ICIs may also exist in patients with EC who exhibit high expression of ZAP70, thus potentially achieving an improved immunotherapeutic effect.

However, after analyzing the clinical data of TCGA-UCEC, it was observed that high expression of ZAP70 was a factor of favorable prognosis in patients with EC. High expression of ZAP70 was found in both early stage and surviving patients. Thus, it was hypothesized that tumorigenesis may activate the immune state of the patient, leading to the phosphorylation and activation of ZAP70, which is a key factor affecting the TCR. High expression of ZAP70 predicts that in patients, immune cells such as T cells and B cells, are sensitive to pMHC on the tumor surface, which results in a good prognosis. In the present study, ZAP70 expression in patients with EC was positively associated with the infiltration of activated CD8<sup>+</sup> T cells. And

the high intraepithelial CD8<sup>+</sup> T cell counts in the endometrium is associated with longer PFS (75). These evidences suggested that ZAP70 may be a good prognostic factor for patients with EC. In the future, we will further study the expression and function of ZAP70 in EC. The present study found that 14 key genes, including ZAP70, may affect the immune micro-environment in patients with EC. The results demonstrated the potential of ZAP70 as a target for EC immunotherapy and may provide new possibilities for immunotherapy in patients with EC.

## Acknowledgements

Not applicable.

## Funding

No funding was received.

## Availability of data and materials

The datasets used and/or analyzed during the current study are available from the corresponding author on reasonable request.

## Authors' contributions

YMZ and YXY designed the project. YMZ and HOL collected data. YMZ performed the experiments. YMZ analyzed the data and wrote the manuscript. All authors read and approved the final version of the manuscript. YMZ, HOL and YXY confirm the authenticity of all the raw data.

## Ethics approval and consent to participate

The present study has been approved by the Ethics Committee of General Hospital of Northern Theater Command (approval no. Y2023002), and the informed consent exemption application has been approved by the Ethics Committee of General Hospital of Northern Theater Command.

## Patient consent for publication

Not applicable.

## Competing interests

The authors declare that they have no competing interests.

## References

- Kalampokas E, Giannis G, Kalampokas T, Papathanasiou AA, Mitsopoulou D, Tsironi E, Triantafyllidou O, Gurumurthy M, Parkin DE, Cairns M and Vlahos NF: Current approaches to the management of patients with endometrial cancer. *Cancers* (Basel) 14: 4500, 2022.
- Hamilton CA, Pothuri B, Arend RC, Backes FJ, Gehrig PA, Soliman PT, Thompson JS, Urban RR and Burke WM: Endometrial cancer: A society of gynecologic oncology evidence-based review and recommendations. *Gynecol Oncol* 160: 817-826, 2021.
- Crosbie EJ, Kitson SJ, McAlpine JN, Mukhopadhyay A, Powell ME and Singh N: Endometrial cancer. *Lancet* 399: 1412-1428, 2022.
- Madariaga A, Coleman RL and González Martín A: Novel therapies leading to a new landscape in gynecologic tumors. *Int J Gynecol Cancer* 33: 321-322, 2023.
- Inoue F, Sone K, Toyohara Y, Tanimoto S, Takahashi Y, Kusakabe M, Kukita A, Honjoh H, Nishijima A, Taguchi A, *et al*: Histone arginine methyltransferase CARM1 selective inhibitor TP-064 induces apoptosis in endometrial cancer. *Biochem Biophys Res Commun* 601: 123-128, 2022.
- Pirš B, Škof E, Smrkolj V and Smrkolj Š: Overview of immune checkpoint inhibitors in gynecological cancer treatment. *Cancers* (Basel) 14: 631, 2022.
- Park JY, Lee JY, Lee YY, Shim SH, Suh DH and Kim JW: Major clinical research advances in gynecologic cancer in 2021. *J Gynecol Oncol* 33: e43, 2022.
- Yanazume S, Iwakiri K, Kobayashi Y, Kitazono I, Akahane T, Mizuno M, Togami S, Tanimoto A and Kobayashi H: Cytopathological features associated with POLE mutation in endometrial cancer. *Cytopathology*: Feb 2, 2023 doi: 10.1111/cyt.13215 (Epub ahead of print).
- Mullen MM and Mutch DG: Endometrial tumor immune response: Predictive biomarker of response to immunotherapy. *Clin Cancer Res* 25: 2366-2368, 2019.
- Rousset-Rouviere S, Rochigneux P, Chrétien AS, Fattori S, Gorvel L, Provansal M, Lambaudie E, Olive D and Sabatier R: Endometrial carcinoma: Immune microenvironment and emerging treatments in immuno-oncology. *Biomedicine* 9: 632, 2021.
- Talhok A, Derocher H, Schmidt P, Leung S, Milne K, Gilks CB, Anglesio MS, Nelson BH and McAlpine JN: Molecular subtype not immune response drives outcomes in endometrial carcinoma. *Clin Cancer Res* 25: 2537-2548, 2019.
- Burke KP, Patterson DG, Liang D and Sharpe AH: Immune checkpoint receptors in autoimmunity. *Curr Opin Immunol* 80: 102283, 2023.
- Izawa M, Tanaka N, Murakami T, Anno T, Teranishi Y, Takamatsu K, Mikami S, Kakimi K, Imamura T, Matsumoto K and Oya M: Single-cell phenotyping of CD73 expression reveals the diversity of the tumor immune microenvironment and reflects the prognosis of bladder cancer. *Lab Invest* 103: 100040, 2023.
- Ashouri JF, Lo WL, Nguyen TTT, Shen L and Weiss A: TZAP70, too little, too much can lead to autoimmunity. *Immunol Rev* 307: 145-160, 2022.
- Chakraborty AK and Weiss A: Insights into the initiation of TCR signaling. *Nat Immunol* 15: 798-807, 2014.
- Leveille E, Chan LN, Mirza AS, Kume K and Müschen M: SYK and ZAP70 kinases in autoimmunity and lymphoid malignancies. *Cell Signal* 94: 110331, 2022.
- Linley AJ and Slupsky JR: Poor prognosis is ZAP70-ed into focus in CLL. *Blood* 137: 3586-3587, 2021.
- Rosenwald A, Alizadeh AA, Widhopf G, Simon R, Davis RE, Yu X, Yang L, Pickeral OK, Rassenti LZ, Powell J, *et al*: Relation of gene expression phenotype to immunoglobulin mutation genotype in B cell chronic lymphocytic leukemia. *J Exp Med* 194: 1639-1647, 2001.
- Au-Yeung BB, Levin SE, Zhang C, Hsu LY, Cheng DA, Killeen N, Shokat KM and Weiss A: A genetically selective inhibitor demonstrates a function for the kinase Zap70 in regulatory T cells independent of its catalytic activity. *Nat Immunol* 11: 1085-1092, 2010.
- Colaprico A, Silva TC, Olsen C, Garofano L, Cava C, Garolini D, Sabedot TS, Malta TM, Pagnotta SM, Castiglioni I, *et al*: TCGAbiolinks: An R/Bioconductor package for integrative analysis of TCGA data. *Nucleic Acids Res* 44: e71, 2016.
- Yan G, An Y, Xu B, Wang N, Sun X and Sun M: Potential Impact of ALKBH5 and YTHDF1 on Tumor Immunity in Colon Adenocarcinoma. *Front Oncol* 11: 670490, 2021.
- Love MI, Huber W and Anders S: Moderated estimation of fold change and dispersion for RNA-seq data with DESeq2. *Genome Biol* 15: 550, 2014.
- Langfelder P and Horvath S: WGCNA: An R package for weighted correlation network analysis. *BMC Bioinformatics* 9: 559, 2008.
- Langfelder P and Horvath S: Eigengene networks for studying the relationships between co-expression modules. *BMC Syst Biol* 1: 54, 2007.
- Yu G, Wang LG, Han Y and He QY: clusterProfiler: An R package for comparing biological themes among gene clusters. *OMICS* 16: 284-287, 2012.
- Reimand J, Isserlin R, Voisin V, Kucera M, Tannus-Lopes C, Rostamianfar A, Wadi L, Meyer M, Wong J, Xu C, *et al*: Pathway enrichment analysis and visualization of omics data using g:Profiler, GSEA, Cytoscape and EnrichmentMap. *Nat Protoc* 14: 482-517, 2019.

27. Szklarczyk D, Gable AL, Lyon D, Junge A, Wyder S, Huerta-Cepas J, Simonovic M, Doncheva NT, Morris JH, Bork P, *et al*: STRING v11: Protein-protein association networks with increased coverage, supporting functional discovery in genome-wide experimental datasets. *Nucleic Acids Res* 47: D607-D613, 2019.
28. Tibshirani R: The lasso method for variable selection in the Cox model. *Stat Med* 16: 385-395, 1997.
29. Wilkerson MD and Hayes DN: ConsensusClusterPlus: A class discovery tool with confidence assessments and item tracking. *Bioinformatics* 26: 1572-1573, 2010.
30. Ritchie ME, Phipson B, Wu D, Hu Y, Law CW, Shi W and Smyth GK: limma powers differential expression analyses for RNA-sequencing and microarray studies. *Nucleic Acids Res* 43: e47, 2015.
31. Yoshihara K, Shahmoradgoli M, Martínez E, Vegesna R, Kim H, Torres-Garcia W, Treviño V, Shen H, Laird PW, Levine DA, *et al*: Inferring tumour purity and stromal and immune cell admixture from expression data. *Nat Commun* 4: 2612, 2013.
32. Newman AM, Liu CL, Green MR, Gentles AJ, Feng W, Xu Y, Hoang CD, Diehn M and Alizadeh AA: Robust enumeration of cell subsets from tissue expression profiles. *Nat Methods* 12: 453-457, 2015.
33. Hänzelmann S, Castelo R and Guinney J: GSVA: Gene set variation analysis for microarray and RNA-seq data. *BMC Bioinformatics* 14: 7, 2013.
34. Livak KJ and Schmittgen TD: Analysis of relative gene expression data using real-time quantitative PCR and the 2(-Delta Delta C(T)) method. *Methods* 25: 402-408, 2001.
35. Greenwood JD, Minhas K, di Santo JP, Makita M, Kiso Y and Croy BA: Ultrastructural studies of implantation sites from mice deficient in uterine natural killer cells. *Placenta* 21: 693-702, 2000.
36. Kolben T, Mannewitz M, Perleberg C, Schnell K, Anz D, Hahn L, Meister S, Schmoekel E, Burges A, Czogalla B, *et al*: Presence of regulatory T-cells in endometrial cancer predicts poorer overall survival and promotes progression of tumor cells. *Cell Oncol (Dordr)* 45: 1171-1185, 2022.
37. Degos C, Heinemann M, Barrou J, Boucherit N, Lambaudie E, Savina A, Gorvel L and Olive D: Endometrial tumor microenvironment alters human NK cell recruitment, and resident NK cell phenotype and function. *Front Immunol* 10: 877, 2019.
38. Wang XQ, Zhou WJ, Luo XZ, Tao Y and Li DJ: Synergistic effect of regulatory T cells and proinflammatory cytokines in angiogenesis in the endometriotic milieu. *Hum Reprod* 32: 1304-1317, 2017.
39. Yu Z, Zhang J, Zhang Q, Wei S, Shi R, Zhao R, An L, Grose R, Feng D and Wang H: Single-cell sequencing reveals the heterogeneity and intratumoral crosstalk in human endometrial cancer. *Cell Prolif* 55: e13249, 2022.
40. Antsiferova YS, Sotnikova NY, Posiseeva LV and Shor AL: Changes in the T-helper cytokine profile and in lymphocyte activation at the systemic and local levels in women with endometriosis. *Fertil Steril* 84: 1705-1711, 2005.
41. Hofmann AP, Gerber SA and Croy BA: Uterine natural killer cells pace early development of mouse decidua basalis. *Mol Hum Reprod* 20: 66-76, 2014.
42. Heikkinen J, Möttönen M, Alanen A and Lassila O: Phenotypic characterization of regulatory T cells in the human decidua. *Clin Exp Immunol* 136: 373-378, 2004.
43. Fu B, Li X, Sun R, Tong X, Ling B, Tian Z and Wei H: Natural killer cells promote immune tolerance by regulating inflammatory TH17 cells at the human maternal-fetal interface. *Proc Natl Acad Sci USA* 110: E231-E240, 2013.
44. Diao R, Wei W, Zhao J, Tian F, Cai X and Duan YG: CCL19/CCR7 contributes to the pathogenesis of endometriosis via PI3K/Akt pathway by regulating the proliferation and invasion of ESCs. *Am J Reprod Immunol*: 78, 2017 doi: 10.1111/aji.12744 (Epub ahead of print).
45. Mei J, Zhou WJ, Zhu XY, Lu H, Wu K, Yang HL, Fu Q, Wei CY, Chang KK, Jin LP, *et al*: Suppression of autophagy and HCK signaling promotes PTGS2high FCGR3-NK cell differentiation triggered by ectopic endometrial stromal cells. *Autophagy* 14: 1376-1397, 2018.
46. Agostinis C, Masat E, Bossi F, Ricci G, Menegazzi R, Lombardelli L, Zito G, Mangogna A, Degan M, Gattei V, *et al*: Transcriptomics and immunological analyses reveal a pro-angiogenic and anti-inflammatory phenotype for decidual endothelial cells. *Int J Mol Sci* 20: 1604, 2019.
47. Hollebecque A, Chung HC, de Miguel MJ, Italiano A, Machiels JP, Lin CC, Dhani NC, Peeters M, Moreno V, Su WC, *et al*: Safety and antitumor activity of  $\alpha$ -PD-L1 antibody as monotherapy or in combination with  $\alpha$ -TIM-3 antibody in patients with microsatellite instability-high/mismatch repair-deficient tumors. *Clin Cancer Res* 27: 6393-6404, 2021.
48. Marabelle A, Le DT, Ascierto PA, Di Giacomo AM, De Jesus-Acosta A, Delord JP, Geva R, Gottfried M, Penel N, Hansen AR, *et al*: Efficacy of pembrolizumab in patients with noncolorectal high microsatellite instability/mismatch repair-deficient cancer: Results from the phase II KEYNOTE-158 study. *J Clin Oncol* 38: 1-10, 2020.
49. Antill Y, Kok PS, Robledo K, Yip S, Cummins M, Smith D, Spurdle A, Barnes E, Lee YC, Friedlander M, *et al*: Clinical activity of durvalumab for patients with advanced mismatch repair-deficient and repair-proficient endometrial cancer. A nonrandomized phase 2 clinical trial. *J Immunother Cancer* 9: e002255: 2021.
50. Chen L, Widhopf G, Huynh L, Rassenti L, Rai KR, Weiss A and Kipps TJ: Expression of ZAP-70 is associated with increased B-cell receptor signaling in chronic lymphocytic leukemia. *Blood* 100: 4609-4614, 2002.
51. Chen L, Apgar J, Huynh L, Dicker F, Giago-McGahan T, Rassenti L, Weiss A and Kipps TJ: ZAP-70 directly enhances IgM signaling in chronic lymphocytic leukemia. *Blood* 105: 2036-2041, 2005.
52. Liu Y, Wang Y, Yang J, Bi Y and Wang H: ZAP-70 in chronic lymphocytic leukemia: A meta-analysis. *Clin Chim Acta* 483: 82-88, 2018.
53. Sun M, Chen S and Fu M: Model establishment of prognostic-related immune genes in laryngeal squamous cell carcinoma. *Medicine (Baltimore)* 100: e24263, 2021.
54. Liu J and Zhang J: T-cell receptors provide potential prognostic signatures for breast cancer. *Cell Biol Int* 45: 1220-1230, 2021.
55. Sun X, Wang L, Li H, Jin C, Yu Y, Hou L, Liu X, Yu Y, Yan R and Xue F: Identification of microenvironment related potential biomarkers of biochemical recurrence at 3 years after prostatectomy in prostate adenocarcinoma. *Aging (Albany NY)* 13: 16024-16042, 2021.
56. Brito C, Costa-Silva B, Barral DC and Pojo M: Unraveling the relevance of ARL GTPases in cutaneous melanoma prognosis through integrated bioinformatics analysis. *Int J Mol Sci* 22: 9260, 2021.
57. Kang Z, Li W, Yu YH, Che M, Yang ML, Len JJ, Wu YR and Yang JF: Identification of Immune-related genes associated with bladder cancer based on immunological characteristics and their correlation with the prognosis. *Front Genet* 12: 763590, 2021.
58. Lyu M, Yi X, Huang Z, Chen Y, Ai Z, Liang Y, Feng Q and Xiang Z: A transcriptomic analysis based on aberrant methylation levels revealed potential novel therapeutic targets for nasopharyngeal carcinoma. *Ann Transl Med* 10: 47, 2022.
59. Jan CI, Huang SW, Canoll P, Bruce JN, Lin YC, Pan CM, Lu HM, Chiu SC and Cho DY: Targeting human leukocyte antigen G with chimeric antigen receptors of natural killer cells convert immunosuppression to ablate solid tumors. *J Immunother Cancer* 9: e003050, 2021.
60. Yin X, He L and Guo Z: T-cell exhaustion in CAR-T-cell therapy and strategies to overcome it. *Immunology*: Mar 20, 2023 doi: 10.1111/imm.13642 (Epub ahead of print).
61. Rowan AG, Ponnusamy K, Ren H, Taylor GP, Cook LBM and Karadimitris A: CAR-iNKT cells targeting clonal TCRV $\beta$  chains as a precise strategy to treat T cell lymphoma. *Front Immunol* 14: 1118681, 2023.
62. Brentjens RJ, Latouche JB, Santos E, Marti F, Gong MC, Lyddane C, King PD, Larson S, Weiss M, Riviere I and Sadelain M: Eradication of systemic B-cell tumors by genetically targeted human T lymphocytes co-stimulated by CD80 and interleukin-15. *Nat Med* 9: 279-286, 2003.
63. Gladkikh AA, Potashnikov DM, Tatarksiy V Jr, Yastrebova M, Khamidullina A, Barteneva N and Vorobjev I: Comparison of the mRNA expression profile of B-cell receptor components in normal CD5-high B-lymphocytes and chronic lymphocytic leukemia: A key role of ZAP70. *Cancer Med* 6: 2984-2997, 2017.
64. Lin JX and Leonard WJ: The common cytokine Receptor  $\gamma$  chain family of cytokines. *Cold Spring Harb Perspect Biol* 10: a028449, 2018.
65. Blanco E, Izotova N, Booth C and Thrasher AJ: Immune reconstitution after gene therapy approaches in patients with X-Linked severe combined immunodeficiency disease. *Front Immunol* 11: 608653, 2020.



66. Le DT, Durham JN, Smith KN, Wang H, Bartlett BR, Aulakh LK, Lu S, Kemberling H, Wilt C, Lubner BS, *et al*: Mismatch repair deficiency predicts response of solid tumors to PD-1 blockade. *Science* 357: 409-413, 2017.
67. Oh MS and Chae YK: Deep and durable response with combination CTLA-4 and PD-1 blockade in mismatch repair (MMR)-proficient endometrial cancer. *J Immunother* 42: 51-54, 2019.
68. Faulkner S, Jobling P, March B, Jiang CC and Hondermarck H: Tumor neurobiology and the war of nerves in cancer. *Cancer Discov* 9: 702-710, 2019.
69. Chen F, Qin T, Zhang Y, Wei L, Dang Y, Liu P and Jin W: Reclassification of endometrial cancer and identification of key genes based on neural-related genes. *Front Oncol* 12: 951437, 2022.
70. Blake MK, O'Connell P and Aldhamen YA: Fundamentals to therapeutics: Epigenetic modulation of CD8+ T Cell exhaustion in the tumor microenvironment. *Front Cell Dev Biol* 10: 1082195, 2022.
71. Philip M and Schietinger A: CD8+ T cell differentiation and dysfunction in cancer. *Nat Rev Immunol* 22: 209-223, 2022.
72. Duckworth BC, Qin RZ and Groom JR: Spatial determinates of effector and memory CD8+ T cell fates. *Immunol Rev* 306: 76-92, 2022.
73. Nelson MA, Ngamcherdtrakul W, Luoh SW and Yantasee W: Prognostic and therapeutic role of tumor-infiltrating lymphocyte subtypes in breast cancer. *Cancer Metastasis Rev* 40: 519-536, 2021.
74. Mestermann K, Giavridis T, Weber J, Rydzek J, Frenz S, Nerretter T, Mades A, Sadelain M, Einsele H and Hudecek M: The tyrosine kinase inhibitor dasatinib acts as a pharmacologic on/off switch for CAR T cells. *Sci Transl Med* 11: eaau5907, 2019.
75. Brunner A, Hinterholzer S, Riss P, Heinze G and Brustmann H: Immunoexpression of B7-H3 in endometrial cancer: Relation to tumor T-cell infiltration and prognosis. *Gynecol Oncol* 124: 105-111, 2012.



This work is licensed under a Creative Commons Attribution-NonCommercial-NoDerivatives 4.0 International (CC BY-NC-ND 4.0) License.